

SUPPLEMENTARY INFORMATION

Indium Silicate with an Imandrite-Type of Structure

Stanislav Ferdov,^{*a} Boris Shivachev,^{*b} Rositsa Titorenkova,^b Nadia Petrova,^b

Mihail Tarassov^b, Rosica Nikolova^b

^[a]Center of Physics of the Universities of Minho and Porto, University of Minho, 4800-058
Guimarães, Portugal

^[b]Institute of Mineralogy and Crystallography, Bulgarian Academy of Sciences, Sofia, 1113,
Bulgaria

*Corresponding authors' e-mail address: sferdov@fisica.uminho.pt; bls@clmc.bas.bg

Table of Contents

1. Scanning electron microscopy (SEM) and quantitative X-ray microanalysis details	3
Table S1. Relative standard errors (ϵ_{p-b} , p – peak, b – background) and p/b for the measured intensities of NaK α , SiK α , CaK α and InL α in the standards used (calculated according to Scott and Love, 1983 ¹)	3
Table S2. Elemental composition of the material according to EDS microanalysis data (wt.%) with indicated standard deviations (+1 σ) of measurement of each component, taking into account the measurement errors of the X-ray lines in the unknown and the standard ($\epsilon^2 = \epsilon_{\text{unknown}}^2 + \epsilon_{\text{STD}}^2$) (relative standard errors and standard deviations were calculated according to Scott and Love, 1983)	3
Figure S1. (a). Morphology of aggregates of intergrown crystals. Unpolished sample. BSE. (b). Cross-section of aggregates of intergrown crystals. All aggregates are characterized by zonal microstructure. Polished sample. BSE.....	4
Figure S2. (a, b). Aggregates of intergrown crystals. Polished samples. BSE images. Rings and numeral symbols in the images indicate the position of points analyzed by EDS. The numeral symbols correspond to the analysis numbers in table 1.	4

Figure S3. The final Rietveld pattern for MS-2. The (+) is the measured values and (green) are the fitted ones; (black -) is the difference between the measured and the fitted values (CSD number 2151073).	5
Figure S4. In situ temperature resolved powder XRD patterns of MS-2 compared with the XRD pattern calculated from the single crystal data.	5
Figure S5. Le Bail fits of the powder XRD patterns collected at different temperatures.	7
Figure S6. Change of the lattice parameters of MS-2 with increasing temperature.....	7
Figure S7. Powder XRD patterns of a) as-synthesized MS-2 and b) after heating at 900 °C.	8
Figure S8. Linear plot of N ₂ (77 K, squares and circles) and CO ₂ (278 and 293 K, triangles) adsorption and desorption isotherms in In-imandrite (MS-2).....	9
Figure S9. Linear plot of N ₂ (77 K, squares and circles) and CO ₂ (278 and 293 K, triangles) adsorption and desorption isotherms in Fe-imandrite (MS-1).	9
Figure S10. Hydrogen adsorption isotherm of and activated carbon (AC) and MS-2 at 77 and 277 K).	10
Table S3. Most important data collection and refinement parameters for the studied sample.	11
Table S4. Comparison of crystal structure parameters of the mineral imandrite, MS-1, and MS-2.....	12
Table S5. Selected bond lengths (Å), for the studied compounds.	13
References	14

1. Scanning electron microscopy (SEM) and quantitative X-ray microanalysis details

SEM/EDS. Scanning electron microscopy (SEM) and quantitative X-ray microanalysis with energy dispersive spectrometer (EDS analysis) were performed by using ZEISS SEM EVO 25LS with an EDAX Trident EDS-EBSD-WDS analysis system (Institute of Mineralogy and Crystallography, BAS). EDS analysis was made at selected points (spot analyses) using an EDAX SDD Apollo 10 EDS detector and Genesis V. 6.2. software with ZAF correction method and albite (for Na, Si), anhydrite (for Ca), metal indium (for In) as standards (Astimex Microanalysis Standards). The EDS spectra of the standards and unknowns were recorded at an acceleration voltage of 18 kV and a probe current of 0.98-1.0 nA using a data collection time of 100-120 live seconds and the following geometry: specimen tilt angle - 0°, working distance - 11.5 mm and X-Ray take-off angle - 37.28°. A correction for electron beam current drift was made for each spectrum using a Faraday cap and measuring the sample current. For SEM/EDS study, the particles of the studied material were fixed in epoxy resin pellet and then polished. Another part of the particles was directly fixed on SEM holders. Then all prepared samples were coated with carbon.

Table S1. Relative standard errors (ϵ_{p-b} , p – peak, b – background) and p/b for the measured intensities of NaK α , SiK α , CaK α and InL α in the standards used (calculated according to Scott and Love, 1983¹)

X-Ray line	$\epsilon_{p-b} * 100\%$	p/b	Standard (Astimex Scientific Ltd)
NaK α	1.05	10.283	Albite NaAlSi ₃ O ₈ Na ₂ O - 11.59 wt.%
SiK α	0.37	57.96	Albite SiO ₂ – 64.03 wt.%
CaK α	0.38	38.81	Anhydrite CaSO ₄ CaO – 41.11 wt.%
InL α	0.30	24.71	Metal In (100 wt.%)

Table S2. Elemental composition of the material according to EDS microanalysis data (wt.%) with indicated standard deviations ($\pm 1\sigma$) of measurement of each component, taking into account the measurement errors of the X-ray lines in the unknown and the standard ($\epsilon^2 = \epsilon_{\text{unknown}}^2 + \epsilon_{\text{STD}}^2$) (relative standard errors and standard deviations were calculated according to Scott and Love, 1983)

N an	Na ₂ O	CaO	In ₂ O ₃	SiO ₂	Sum	Na	Ca	In	Si	Si/In atomic ratio
	Oxides, wt.%					Atoms per formula unit				
1. dark	27.54 +0.34	12.65 +0.12	12.22 +0.16	49.26 +0.29	101.67	13.006 +0.161	3.300 +0.031	1.288 +0.017	12 +0.071	9.32±0.13
2. dark	25.76 +0.31	13.50 +0.11	11.09 +0.14	49.86 +0.27	100.21	12.018 +0.145	3.482 +0.028	1.156 +0.015	12 +0.064	10.38±0.15
3. light	26.32 +0.33	9.93 +0.10	14.92 +0.17	47.97 +0.28	99.14	12.765 +0.160	2.661 +0.027	1.617 +0.018	12 +0.070	7.42±0.09
4. dark	25.88 +0.32	13.30 +0.11	11.88 +0.15	49.59 +0.28	100.66	12.142 +0.152	3.447 +0.028	1.244 +0.016	12 +0.068	9.65±0.14
5. light	28.00 +0.35	10.38 +0.10	14.61 +0.17	49.10 +0.28	102.10	13.265 +0.166	2.719 +0.026	1.544 +0.018	12 +0.070	7.77±0.10

6. centrum	19.34 +0.26	6.80 +0.08	19.09 +0.19	49.99 +0.28	95.22	8.997 +0.121	1.749 +0.021	1.982 +0.020	12 +0.067	6.05+0.07
7. light	27.20 +0.34	10.05 +0.10	14.79 +0.17	48.54 +0.28	100.58	13.039 +0.163	2.663 +0.026	1.582 +0.018	12 +0.069	7.59+0.10
8. light	26.43 +0.33	10.85 +0.10	14.07 +0.16	48.03 +0.27	99.39	12.803 +0.160	2.906 +0.027	1.523 +0.017	12 +0.067	7.88+0.10
9. dark	26.49 +0.33	12.59 +0.11	11.80 +0.16	48.53 +0.28	99.41	12.699 +0.158	3.334 +0.029	1.263 +0.017	12 +0.069	9.50+0.14
10. light	27.26 +0.33	11.47 +0.10	13.58 +0.14	48.78 +0.26	101.09	13.006 +0.157	3.023 +0.026	1.446 +0.015	12 +0.064	8.30+0.10
11. dark	26.72 +0.34	13.13 +0.12	11.42 +0.15	49.32 +0.28	100.59	12.605 +0.160	3.423 +0.031	1.201 +0.016	12 +0.068	9.99+0.14

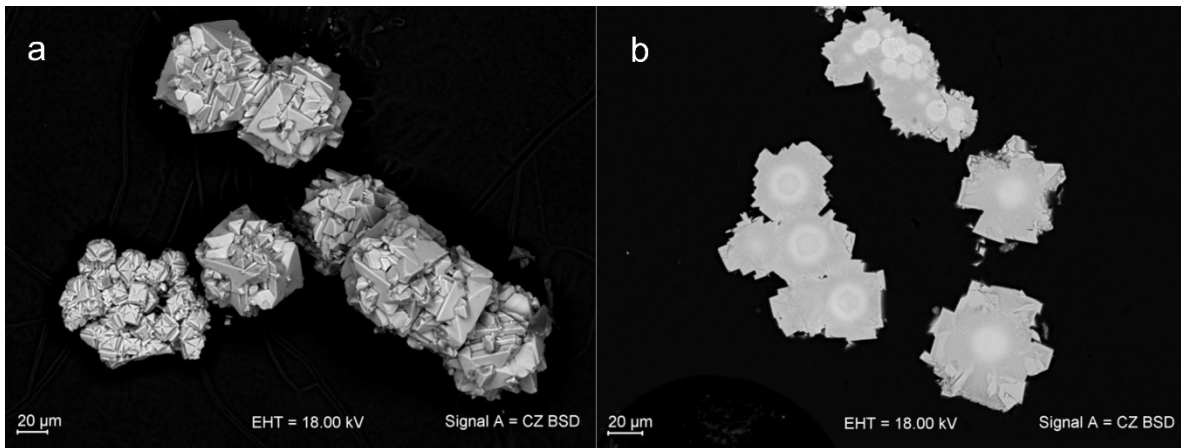


Figure S1. (a). Morphology of aggregates of intergrown crystals. Unpolished sample. BSE. (b). Cross-section of aggregates of intergrown crystals. All aggregates are characterized by zonal microstructure. Polished sample. BSE.

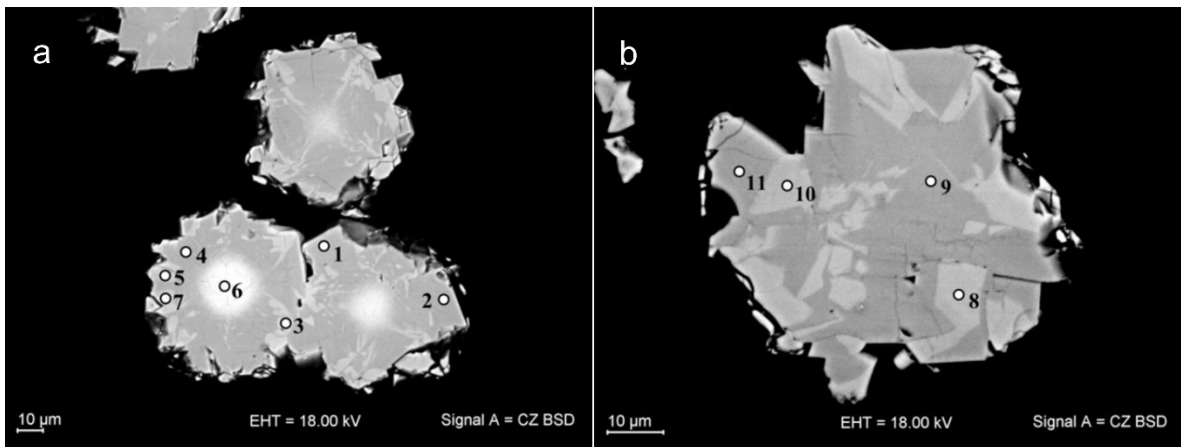


Figure S2. (a, b). Aggregates of intergrown crystals. Polished samples. BSE images. Rings and numeral symbols in the images indicate the position of points analyzed by EDS. The numeral symbols correspond to the analysis numbers in table 1.

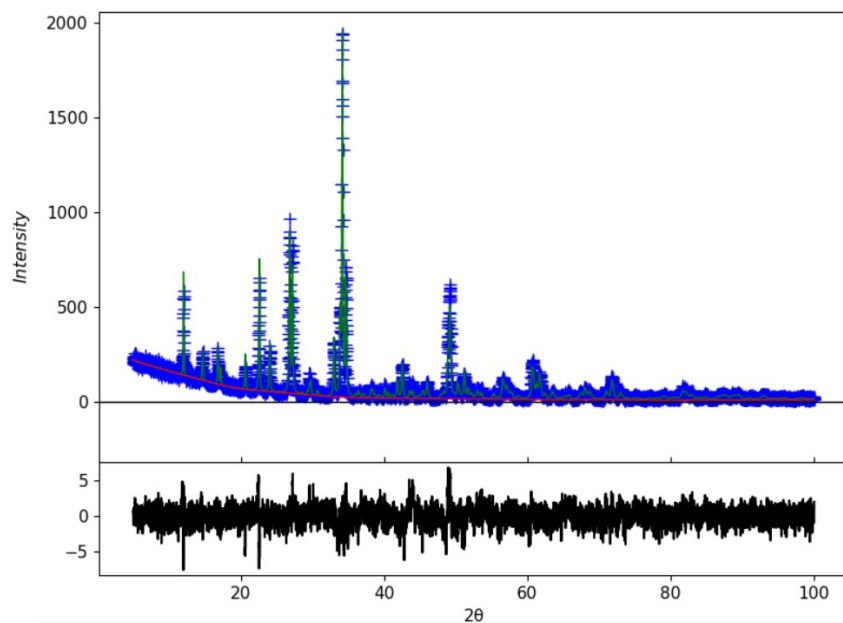


Figure S3. The final Rietveld pattern for MS-2. The (+) is the measured values and (green) are the fitted ones; (black -) is the difference between the measured and the fitted values (CSD number 2151073).

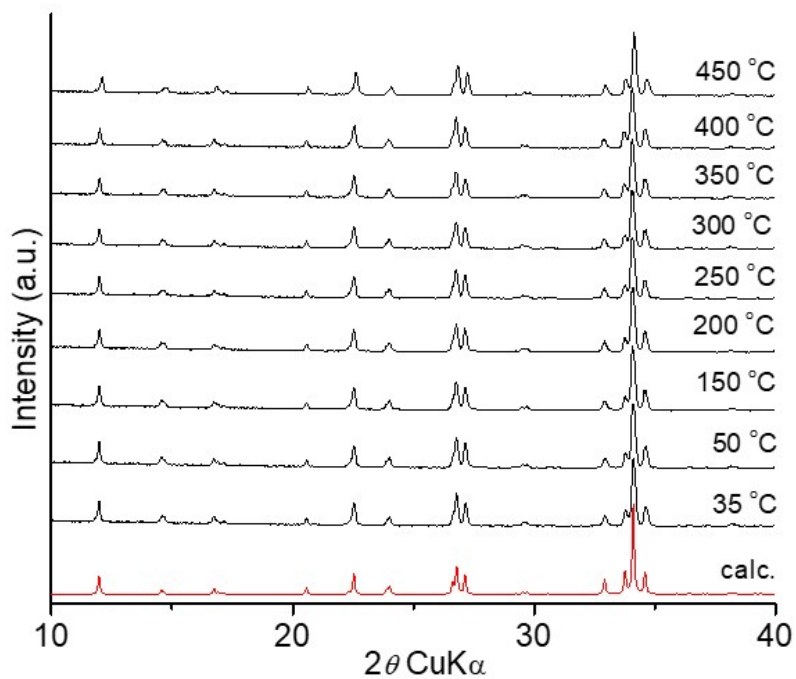
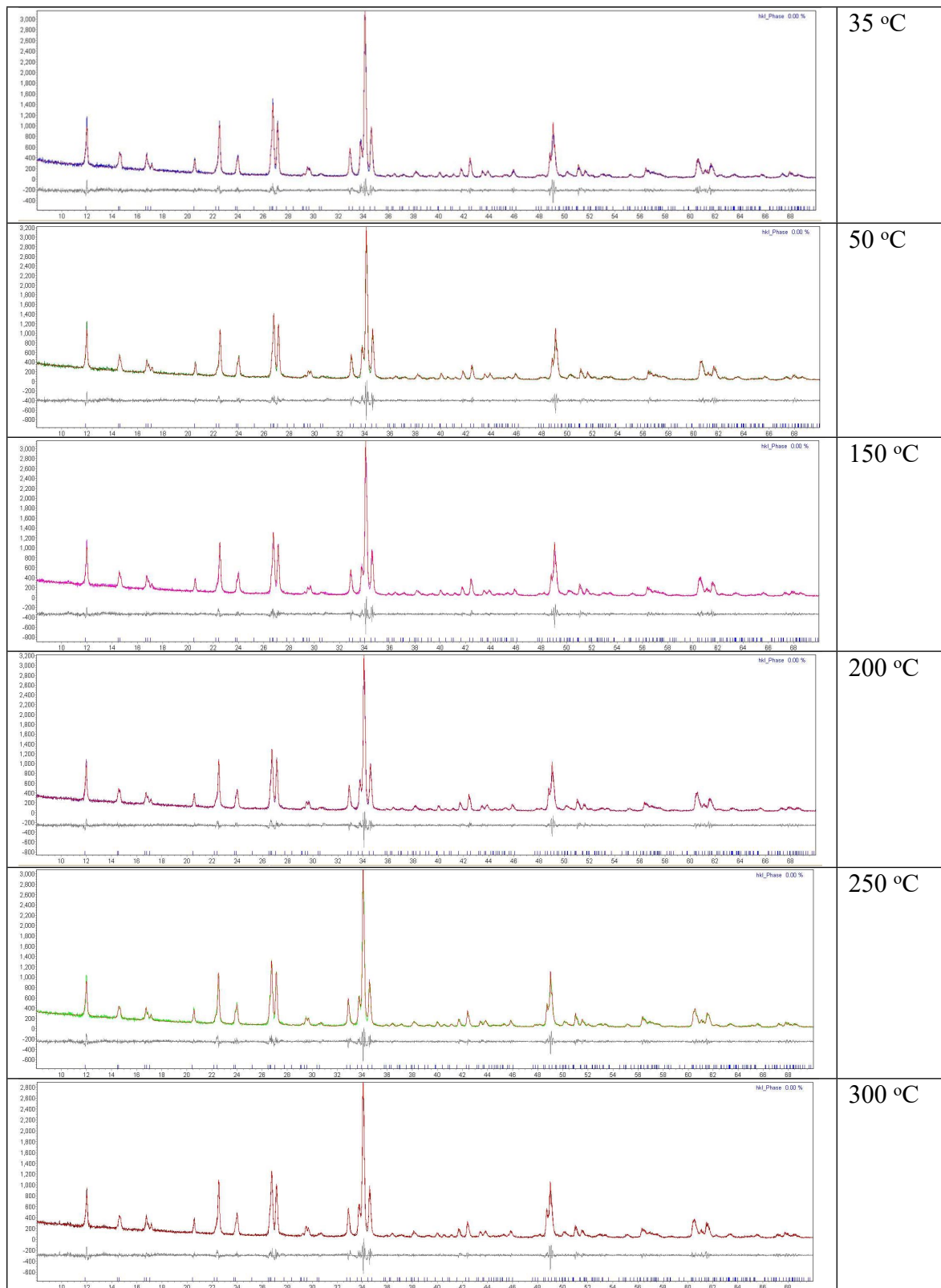


Figure S4. In situ temperature resolved powder XRD patterns of MS-2 compared with the XRD pattern calculated from the single crystal data.



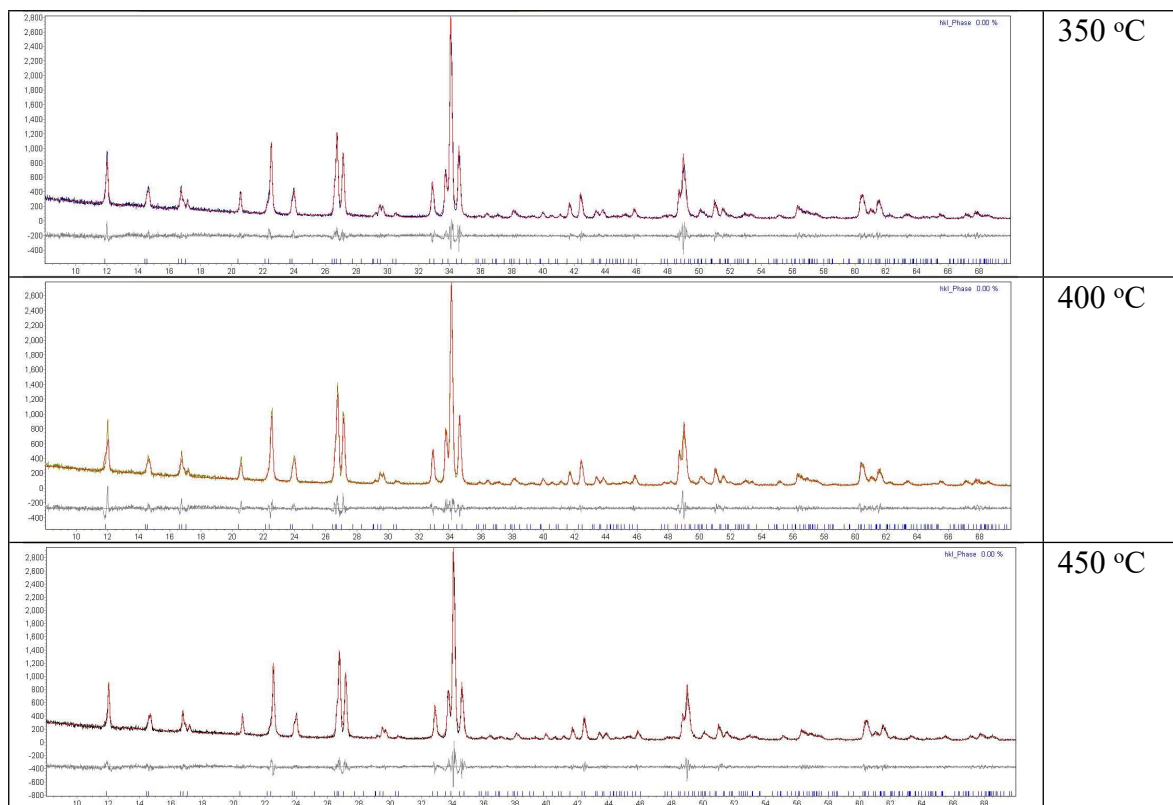


Figure S5. Le Bail fits of the powder XRD patterns collected at different temperatures.

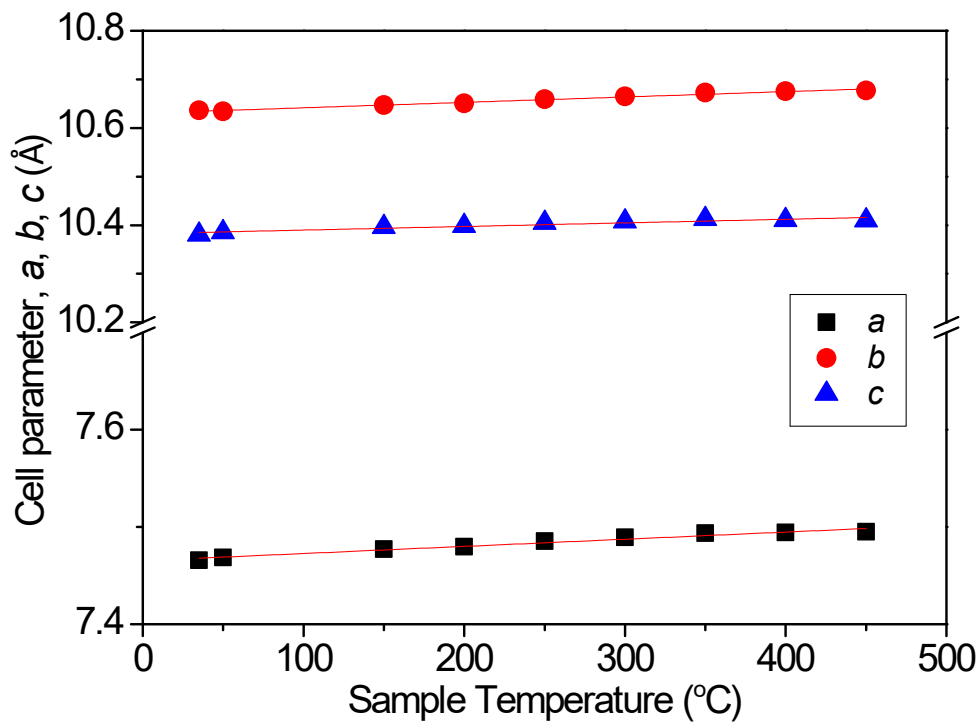


Figure S6. Change of the lattice parameters of MS-2 with increasing temperature.

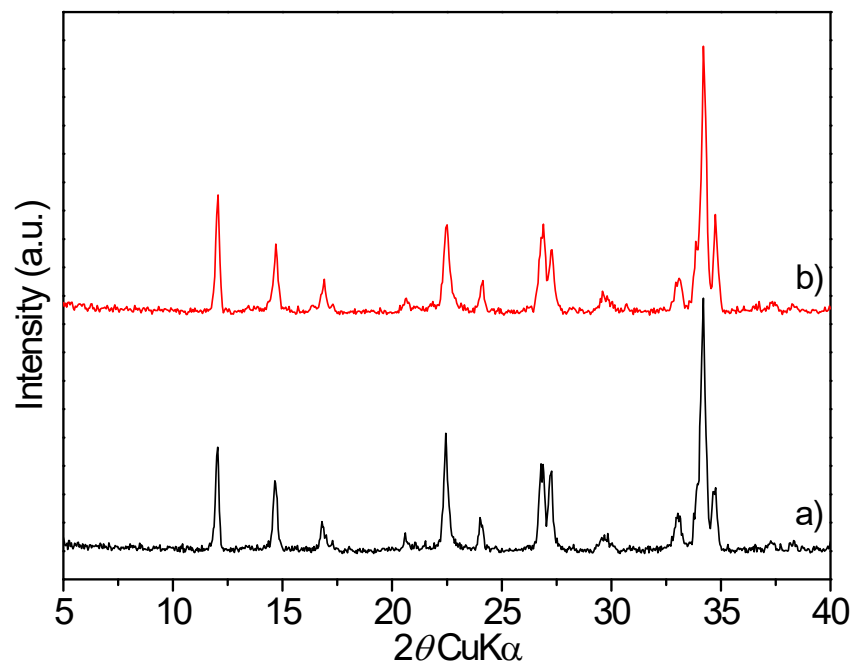


Figure S7. Powder XRD patterns of a) as-synthesized MS-2 and b) after heating at 900 °C.

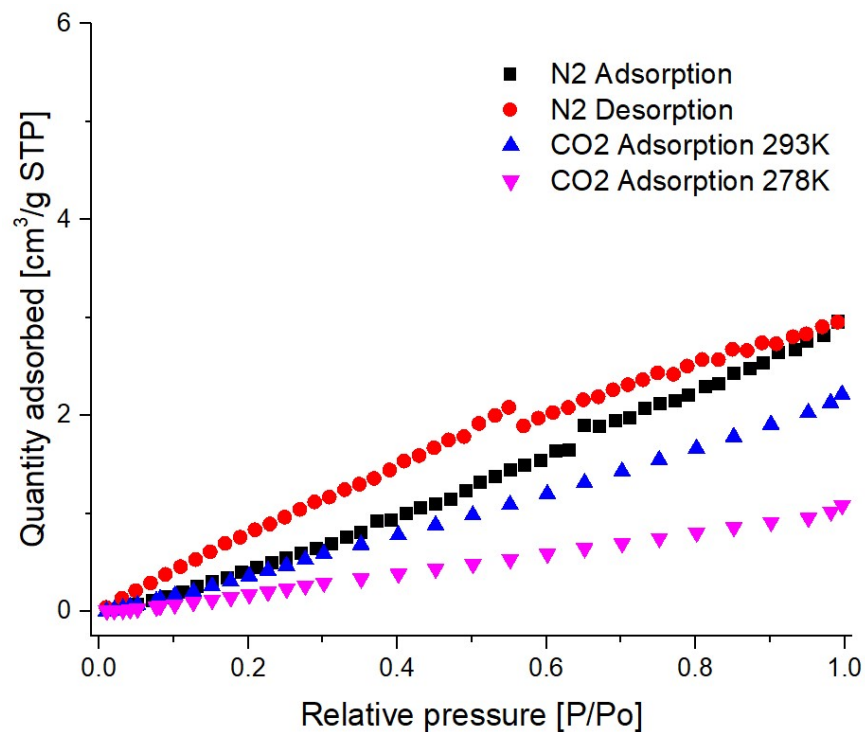


Figure S8. Linear plot of N₂ (77 K, squares and circles) and CO₂ (278 and 293 K, triangles) adsorption and desorption isotherms in In-imandrite (MS-2).

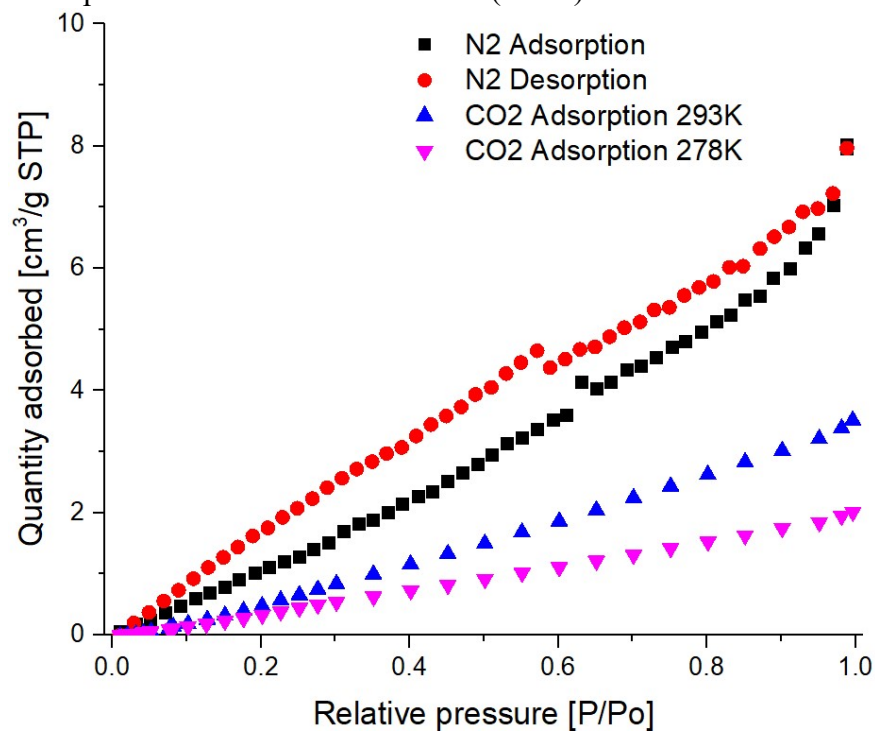


Figure S9. Linear plot of N₂ (77 K, squares and circles) and CO₂ (278 and 293 K, triangles) adsorption and desorption isotherms in Fe-imandrite (MS-1).

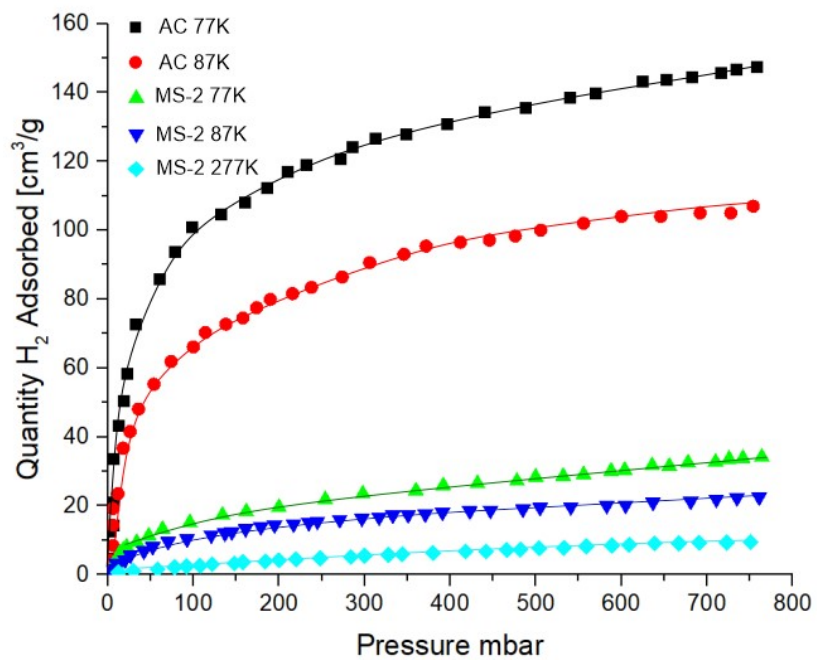


Figure S10. Hydrogen adsorption isotherm of and activated carbon (AC) and MS-2 at 77 and 277 K).

Table S3. Most important data collection and refinement parameters for the studied sample.

Compound	MS-2
Chemical formula	Na _{6.23} Ca _{1.62} In _{0.68} Si ₆ O ₁₈
Formula weight	743.55
Temperature/K	290(2)
Crystal color	White / colorless
Crystal system	Orthorhombic
Space group	<i>P n n m</i>
<i>a</i> /Å	7.4634(5)
<i>b</i> /Å	10.6336(9)
<i>c</i> /Å	10.3869(7)
$\alpha = \beta = \gamma/^\circ$	90
Volume/Å ³	824.33(10)
<i>Z</i>	2
ρ_{calc} (mg/cm ³)	2.996
μ/mm^{-1}	2.213
<i>F</i> (000)	725
Crystal size/mm ³	0.01×0.01×0.01
Radiation, λ [Å]	MoK α , $\lambda = 0.71073$
Θ range for data collection/ $^\circ$	2.741 to 26.370
Limiting indices	-9 $\leq h \leq$ 9, -13 $\leq k \leq$ 13, -12 $\leq l \leq$ 12
Reflections collected /unique	11991 / 890 [<i>R</i> (int) = 0.0738]
Completeness to theta = 25.242	99.6 %
Refinement method	Full-matrix least-squares on <i>F</i> ²
Data/restraints/parameters	890 / 0 / 96
Goodness-of-fit on <i>F</i> ²	1.146
Final <i>R</i> indexes [<i>I</i> \geq 2 σ (<i>I</i>)]	<i>R</i> 1 = 0.0395, <i>wR</i> 2 = 0.0742
Final <i>R</i> indexes [all data]	<i>R</i> 1 = 0.0458, <i>wR</i> 2 = 0.0766
Largest diff. peak/hole /e Å ⁻³	0.545/-0.560

Table S4. Comparison of crystal structure parameters of the mineral imandrite, MS-1, and MS-2.

	Imandrite natural	MS-1	MS-2
Chemical composition	$\text{Na}_6\text{Ca}_{1.5}\text{FeSi}_6\text{O}_{18}$	$\text{Na}_{6.74}\text{Ca}_{1.25}\text{FeSi}_6\text{O}_{18}$	$\text{Na}_{6.23}\text{Ca}_{1.62}\text{In}_{0.68}\text{Si}_6\text{O}_{18}$
FW		717.84	744.93
SG	<i>P n n m</i>	<i>P n n m</i>	<i>P n n m</i>
<i>a</i> (Å)	7.426	7.4041(12)	7.4634(8)
<i>b</i> (Å)	10.546	10.5166(19)	10.6365(11)
<i>c</i> (Å)	10.331	10.307(3)	10.3840(11)
<i>V</i> (Å ³)	809.068	802.5(3)	824.33(15)
FD (FC/1000 Å ³)		18	16.98 / 16.22
Dx, g.cm ⁻³		2.971	2.996

Table S5. Selected bond lengths (Å), for the studied compounds.

MS-2		MS-1	
bond	(Å)	bond	(Å)
Si(1)-O(3)	1.6270(13)	Si(1)-O(2)	1.611(5)
Si(1)-O(4)	1.637(3)	Si(1)-O(4)	1.580(5)
Si(1)-O(5)	1.603(3)	Si(1)-O(5)	1.642(2)
Si(1)-O(6)	1.570(3)	Si(1)-O(6)	1.647(5)
Si(2)-O(1)	1.585(4)	Si(2)-O(1)	1.603(6)
Si(2)-O(2)	1.585(4)	Si(2)-O(3)	1.578(6)
Si(2)-O(4)x2	1.590(4)	Si(2)-O(6)x2	1.648(5)
In-O(2)x2	2.245(4)	Fe-O(1)x2	2.098(6)
In-O(5)x4	2.222(3)	Fe-O(2)x4	2.075(5)
M(1)-O(2)x4	2.653(3)	Na(1)-O(2)x4	2.719(5)
M(1)-O(3)x2	2.269(4)	Na(1)-O(3)x2	2.266(6)
M(1)-O(5)x2	2.608(3)	Na(1)-O(5)x2	2.450(8)
M(2)-O(1)	2.424(4)	Na(2)-O(1)	2.426(6)
M(2)-O(2)x2	2.491(3)	Na(2)-O(2)x2	2.480(5)
M(2)-O(3)	2.386(4)	Na(2)-O(3)	2.335(6)
M(2)-O(4)x2	2.304(3)	Na(2)-O(4)x2	2.257(5)
Na(1)-O(4) x 4	2.632(4)	Na(4)-O(4) x 4	2.688(6)
Na(1)-O(6) x 4	2.686(4)	Na(4)-O(6) x 4	2.683(5)
Na(2)-O(1)	2.768(2)	Na(3)-O(1)	2.607(3)

Na(2)-O(2)	2.613(2)	Na(3)-O(2)	2.561(5)
Na(2)-O(3)	2.8069(17)	Na(3)-O(3)	2.742(3)
Na(2)-O(4)	2.793(3)	Na(3)-O(4)	2.294(5)
Na(2)-O(4)	2.488(4)	Na(3)-O(4)	2.586(6)
Na(2)-O(5)	2.607(4)	Na(3)-O(5)	2.794(3)
Na(2)-O(6)	2.313(4)	Na(3)-O(6)	2.508(6)
Na(2)-O(6)	2.633(4)	Na(3)-O(6)	2.682(6)

M1 = Ca1, Na11; **M2**=Ca2 Na21

References

1. Scott, V.D. and Love, G. (Eds), Quantitative electron-probe microanalysis. 1983, 345 p. (Ellis Horwood Ltd).